Relaxometric, Structural, and Dynamic NMR Studies of DOTA-like Ln(III) Complexes (Ln = La, Gd, Ho, Yb) Containing a *p*-Nitrophenyl Substituent

Silvio Aime,*,† Mauro Botta,† Giuseppe Ermondi,† Enzo Terreno,† Pier Lucio Anelli,‡ Franco Fedeli,‡ and Fulvio Uggeri‡

Dipartimento di Chimica Inorganica, Chimica Fisica e Chimica dei Materiali, Università di Torino, Via P. Giuria 7, I-10125 Torino, Italy, and Bracco S.p.A., Via E. Folli 50, I-20134 Milano, Italy

Received July 28, 1995[⊗]

We report here the synthesis of the ligand 1-((*p*-nitrophenyl)carboxymethyl)-4,7,10-tris(carboxymethyl)-1,4,7,-10-tetraazacyclododecane (**3**) and its La(III), Gd(III), Ho(III), and Yb(III) complexes. The introduction of the *p*-nitrophenyl substituent on the methylenic carbon of one acetate group does not alter the overall chelating ability of **3** with respect to the parent DOTA ligand. The [Gd(**3**)]$^-$ complex displays a slightly higher relaxivity than that of [Gd(DOTA)]$^-$, mainly as a consequence of a longer molecular reorientational correlation time (τ_R), due to the increased molecular dimension of the complex, and of limited changes to the other relaxation parameters. A further increase of relaxivity has been observed upon formation of an inclusion compound with β-cyclodextrin. The solution structure and dynamics were thoroughly investigated by high-resolution NMR spectroscopy. Of the four possible enantiomeric pairs that could be present in the solutions of monosubstituted derivatives of [Ln(DOTA)]$^-$ complexes, the proton spectra of Ho and Yb derivatives are consistent with the occurrence of only two isomeric species whose structures have been elucidated through analysis of dipolar shifts and 2D-EXSY data. In both species the bulky aromatic group has replaced the acetate proton pointing outward from the coordination cage. Unlike in the DOTA case, in [Ln(**3**)]$^-$ complexes the isomerization process involves the inversion of the ethylenic groups of the macrocycle rather than the motion of the acetate arms. This behavior is rationalized in terms of steric crowding at the substituent site: minimization of the steric interactions between the aromatic group and the macrocyclic ring protons results in both structural and dynamic selectivity. Interestingly, in the case of the diamagnetic La(III) complex the variable temperature behavior of the ^{13}C NMR spectra is consistent with an exchange process involving one major species and at least one minor isomer of very low concentration, whose relative population increases with temperature. This causes a persistent exchange broadening of the resonances over a wide range of temperatures.

Introduction

Very high thermodynamic and kinetic stability[1,2] coupled with a favorable, long electronic relaxation time[3,4] (τ_S) makes [Gd(DOTA)]$^-$ a superb prototype of a contrast agent (CA) for magnetic resonance imaging (MRI). Currently the search for new CAs which display increased selectivity toward organs and tissues is based, as far as possible, on maintaining these peculiar properties. Thus, one may envisage a possible route to a new generation of CAs that involves introducing suitable functionalities on the surface of a [Gd(DOTA)]$^-$ structure. Previous work dealing with the transformation of an acetate into a functionalized amide group showed that such a change is accompanied by a drastic shortening of the electronic relaxation time of the Gd(III) ion.[5] This undesirable feature is due to changes in the coordination cage when the oxygen of a carboxylate functionality is substituted by a carboxamido donor group as shown in other cases involving amide derivatives of linear[6] and cyclic[7] polyamino carboxylate Gd(III) complexes. To limit such effects an alternative approach may be pursued by introducing the substituent on the methylenic carbon of the acetate group.

Another point of interest in the study of these DOTA-like Ln(III) complexes is associated with the assessment of their solution structures and dynamics. The solid state X-ray structures determined for DOTA complexes of Eu,[8] Gd,[9] Y,[9,10] Ho,[11] and Lu[11] have shown that the lanthanide chelates are isostructural with the octadentate macrocyclic ligand arranged about the metal ion to give a square antiprismatic coordination geometry. The twist angle between the two square planes is about 39°. We have recently shown[12] that in solution the complexes are present in two isomeric forms differing essentially in the layout of the acetate arms but displaying an identical staggered conformation of the macrocyclic ring. The coordination polyhedron of the second isomer can be described as an "inverted" square antiprism where the twist angle between the

* Corresponding author. Telephone: (+39)-11-6707520. FAX: (+39)-11-6707524. E-mail: aime@silver.ch.unito.it.
† Università di Torino.
‡ Bracco S.p.A.
⊗ Abstract published in *Advance ACS Abstracts,* April 1, 1996.

(1) Wang, X.; Jin, T.; Comblin, V.; Lopez-Mut, A.; Merciny, E.; Desreux, J. F. *Inorg. Chem.* **1992**, *31*, 1095.
(2) Toth, E.; Brücher, E.; Lazar, I.; Toth, I. *Inorg. Chem.* **1994**, *33*, 4070.
(3) Koenig, S. H.; Brown, R. D., III. *Prog. NMR Spectrosc.* **1990**, *22*, 487.
(4) Aime, S.; Botta, M.; Ermondi, G.; Fedeli, F.; Uggeri, F. *Inorg. Chem.* **1992**, *31*, 1100.
(5) Sherry, A. D.; Brown, R. D., III; Geraldes, C. F. G. C.; Koenig, S. H.; Kuan, K.-T.; Spiller, M. *Inorg. Chem.* **1989**, *28*, 620.
(6) Aime, S.; Botta, M.; Fasano, M.; Paoletti, S.; Anelli, P. L.; Uggeri, F.; Virtuani, M. *Inorg. Chem.* **1994**, *33*, 4707.
(7) Aime, S.; Anelli, P. L.; Botta, M.; Fedeli, F.; Grandi, M.; Paoli, P.; Uggeri, F. *Inorg. Chem.* **1992**, *31*, 2422.
(8) Spirlet, M. R.; Rebizant, J.; Desreux, J. F.; Loncin, F. *Inorg. Chem.* **1984**, *23*, 359.
(9) Chang, C. A.; Francesconi, L. C.; Malley, M. F.; Kumar, K.; Gougoutas, J. Z.; Tweedle, M. F.; Lee, D. W.; Wilson, L. J. *Inorg. Chem.* **1993**, *32*, 3501.
(10) Parker, D.; Pulukkody, K.; Smith, F. C.; Batsanov, A.; Howard, J. A. K. *J. Chem. Soc., Dalton Trans.* **1994**, 689.
(11) Aime, S.; Botta, M.; Bombieri, G. *Inorg. Chim. Acta*, in press.
(12) Aime, S.; Botta, M.; Ermondi, G. *Inorg. Chem.* **1992**, *31*, 4291.

S0020-1669(95)00981-5 CCC: $12.00

Chart 1

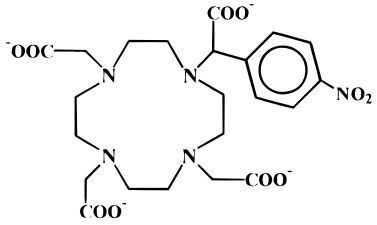

two square planes is about 23°. The substitution of one of the two nonequivalent acetate protons for a Y-group can be expected to affect the number of isomeric species in solution and their interconversion processes.

To investigate all these different aspects we synthesized the *p*-nitrophenyl derivative of the DOTA ligand (**3**; Chart 1), a lanthanide chelator recently described by Cheng *et al.*,[13] and its complexes with diamagnetic (La) and paramagnetic (Gd, Ho, and Yb) ions. Furthermore the NO_2 substituent on the para carbon of the phenyl group represents a potential site for further modification of the paramagnetic probe. This represents a means of improving the specificity towards desired target tissues, a requirement of increasing importance in diagnostic and therapeutic applications of metal chelates.

Experimental Section

Electrodialyses were carried out with an instrument, model ED 0.004 from Hydro Air Research (Zerbo di Opera, Milan, Italy), fitted with seven cation- and five anion-exchange STX membranes (total exchange surface: 0.004 m^2) and operated at 12 V. HPLC analyses were performed on a Merck-Hitachi Lichrograph modular liquid chromatograph using the following methods: (A) E. Merck Lichrospher 100 RP-8 column, 5 μm, 250 × 4 mm, thermostated at 40 °C; eluent, 30% MeCN 70% 0.017 M aqueous H_3PO_4; flow rate, 1.0 mL/min; UV, 280 nm; (B) E. Merck Lichrospher 100 RP-8 column, 5 μm, 250 × 4 mm, thermostated at 40 °C; eluent, 5% MeCN 95% 0.017 M aqueous H_3PO_4; flow rate, 1.0 mL/min; UV, 280 nm. ^{1}H NMR and ^{13}C NMR spectra were recorded on Bruker AC 200, JEOL EX-90, and JEOL EX-400 spectrometers. The ^{1}H NMR spectrum of **2** is not reported because the broad and overlapping resonances are of no use for the structural assignment. Elemental analyses within commonly accepted limits (H, ±0.2%; C, N, Ln, Na, ±0.4%) were obtained for all new compounds.

Organic and inorganic reagents were purchased from E. Merck, Darmstadt, Germany, and used without further purification. $LaCl_3$, $GdCl_3 \cdot 6H_2O$, $HoCl_3 \cdot 6H_2O$, and $YbCl_3 \cdot 6H_2O$ were obtained from Aldrich (Milan, Italy).

α-Bromo-4-nitrobenzeneacetic acid (1) was prepared from 4-nitrobenzeneacetic acid following the general methodology for α-bromination reported by Harpp *et al.*[14] *Caution* must be used in handling the title compound as it is highly vescicating!

α-(*p*-Nitrophenyl)-1,4,7,10-tetraazacyclododecane-1-acetic Acid Trishydrobromide (2). A solution of **1** (233.5 g, 0.8 mol) in CH_2Cl_2 (1.6 L) was dripped over 2 h into a stirred solution of 1,4,7,10-tetraazacyclododecane (275.2 g, 1.6 mol) in H_2O (1.6 L) maintained at 15−20 °C in an ice-water bath. After being stirred for 2 h at 20 °C the organic phase was separated. The aqueous phase was washed with CH_2Cl_2 (2 × 100 mL) and acidified with 47% HBr (320 mL) to give an amorphous precipitate. This was decanted and the aqueous phase washed with CH_2Cl_2 (3 × 150 mL) and concentrated (to 1 kg). Addition of EtOH (2.5 L) led to the precipitation of a white solid (1,4,7,10-tetraazacyclododecane trihydrobromide, 197 g). The solution was concentrated to eliminate EtOH and the residue diluted with H_2O (to 1 kg). Acidification with 47% HBr (750 mL) gave a precipitate which was filtered and dissolved in H_2O (2.5 L). A small amount of insoluble solid was filtered off. The solution was concentrated (to 1 kg) to give a precipitate which was crystallized several times from H_2O. After drying *in vacuo* (KOH, 2 kPa, 50 °C) **2** (285 g; 60%) was obtained as an orange solid: mp 236 °C (dec); HPLC (method A) retention time, 4.8 min (purity, 98.4%);^{13}C NMR (D_2O + NaOD) 45.7, 46.4, 48.1, 50.5, 71.6, 126.6, 133.7, 147.4, 149.7, 160.3.

1-((*p*-Nitrophenyl)carboxymethyl)-4,7,10-tris(carboxymethyl)-1,4,7,10-tetraazacyclododecane (3). A suspension of **2** (200.6 g, 0.34 mol) and bromoacetic acid (183.4 g, 1.32 mol) in H_2O (500 mL), cooled to 15−20 °C with an ice-water bath, was adjusted to pH 10 by slow addition (80 min) of 5 N NaOH (650 mL). The reaction mixture was maintained at pH 10 (by addition of 5 N NaOH by means of a pH-stat apparatus) and room temperature for 4 h. Acidification (pH 2.5) of the reaction mixture with 47% HBr gave a yellow precipitate which was filtered and washed with H_2O (600 mL) and MeOH (2 × 1 L). The solid was dissolved in 1 N NaOH (550 mL) and the solution dripped into H_2O (500 mL) containing 47% HBr (66 mL). The pH was adjusted to 2.5 with NaOH and the precipitate then filtered and washed with H_2O (2 × 1.5 L). After drying, the solid (crude **3**, 156 g, 86% by HPLC, containing NaBr, 8.4%) was dissolved in H_2O (12 L) and loaded onto a column of Amberlite IR 120 (12 L, H^+ form). This was eluted first with H_2O and then with 2.5 N NH_4OH. The alkaline solution was evaporated to dryness and the residue dissolved in H_2O and evaporated. This procedure was repeated three times. The residue was dissolved in H_2O (6 L) and the solution acidified to pH 3.2 by addition of Amberlite IR 120 resin (200 mL, H^+ form). After filtration, the solution was loaded onto a column of Amberlite XAD 2 (400 mL) which was eluted with H_2O. The eluted solution was concentrated and dried (P_2O_5, 2 kPa, 40 °C) to yield **3** (50.3 g; 28%) as an orange solid: mp 131 °C (dec); HPLC (method B) retention time, 6.5 min (purity, 99%); ^{13}C NMR (D_2O + DCl) 44.9, 47.1, 48.9, 50.6, 52.4, 53.0, 53.8, 54.6, 55.4, 56.2, 64.4, 125.6, 132.8, 140.4, 149.1, 169.2, 169.6, 174.1, 175.9.

Complexation Procedure. Ligand **3** (2.1 g, 4 mmol) was suspended in H_2O (20 mL) and solubilized by addition of 2 N NaOH (4 mL). A solution of lanthanide trichloride (4 mmol) in H_2O (10 mL) was added and the pH slowly adjusted to 6.5 and maintained at this value by addition of 2 N NaOH using a pH-stat apparatus. After 10 h the solution was filtered through a 0.45 μm filter and desalted by electrodialysis. The pH of the solution was adjusted to 6.5 with 1 N NaOH. The solvent was then evaporated and the residue dried (P_2O_5, 50 °C, 2 kPa).

Na[La(3)]. Yield 69%. White solid, mp >250 °C; HPLC (method B) retention time, 31.0 min (purity, 97.8%).

Na[Gd(3)]. Yield 66%. White solid, mp >250 °C; HPLC (method B) retention time, 24.0 min (purity, 98.4%).

Na[Ho(3)]. Yield 66%. White solid, mp >250 °C; purity >95% (by ^{1}H NMR).

Na[Yb(3)]. Yield 66%. White solid, mp >250 °C; HPLC (method B) retention time, 19.6 min (purity, 98.7%).

NMR Measurements. The variable temperature longitudinal solvent proton relaxation rates were obtained for 1−2 mM solutions of $[Gd(\mathbf{3})]^-$ on a Stelar Spinmaster spectrometer (Stelar, Mede (PV), Italy) operating at 20 MHz, by means of the standard inversion−recovery technique (16 experiments, 4 scans). A typical 90° pulse width was 3.5 μs and the reproducibility of T_1 data was ±0.5%. The variable field relaxation rates were acquired with a field cycling Koenig−Brown relaxometer (University of Florence, Italy) which operates over a continuum of magnetic field strengths from 2.5×10^{-4} to 1.4 T (corresponding to 0.01−50 MHz proton Larmor frequencies). Details of the instrument and of the data acquisition procedure are given elsewhere.[15] Samples for high-resolution measurements were prepared in D_2O (99.95%; Merck, Germany) at 50−80 mM concentrations. A drop of *tert*-butyl alcohol was added to the solution in the NMR tube as an internal chemical shift reference (δ_H = 0.0 ppm; δ_C = 31.3 ppm).

Results and Discussion

Synthesis of Ligand 3 and $[Ln(3)]^-$ Complexes. Ligand **3** was synthesized according to Scheme 1. The procedure for

(13) Cheng, R.; et al. Dow Chemical Co. WO 89/12631; 28 Dec 1989.
(14) Harpp, D. N.; Bao, L. Q.; Black, C. J.; Gleason, J. G.; Smith, R. A. *J. Org. Chem.* **1975**, *40*, 3420.
(15) Koenig, S. H.; Brown, R. D., III. *NMR Spectroscopy of Cells and Organisms*; Gupta, R. K., Ed.; CRC Press: Boca Raton, 1987; Vol. II.

Scheme 1[a]

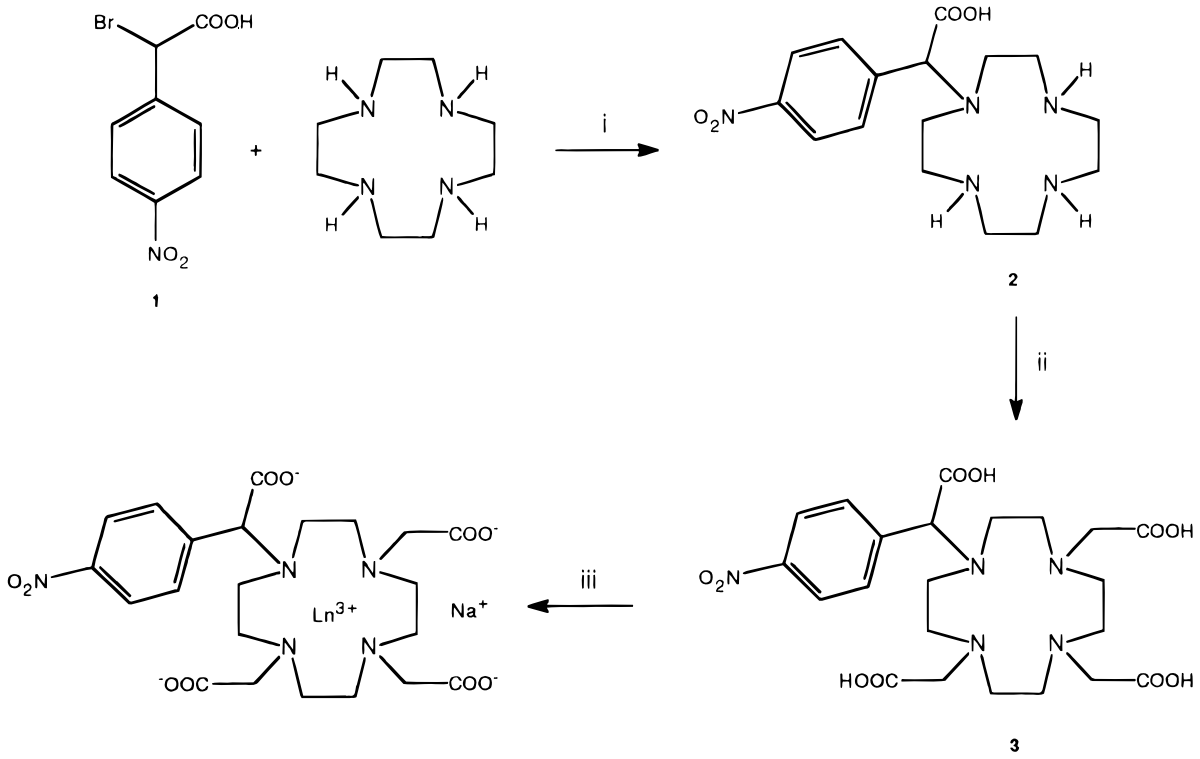

[a] (i) $H_2O-CH_2Cl_2$, room temperature. (ii) $BrCH_2COONa$, H_2O (pH 10), room temperature (iii) $LnCl_3$, H_2O (pH 6.95).

α-bromination of carboxylic acids, as reported by Harpp *et al.*,[14] was used for the preparation of α-bromo-4-nitrobenzeneacetic acid (**1**). Monoalkylation of 1,4,7,10-tetraazacyclododecane with **1** was achieved in fairly good yield using a 100% excess of the macrocycle in a two-phase ($CH_2Cl_2-H_2O$) reaction medium. Carboxymethylation of **2** with bromoacetic acid in water at pH 10 gave ligand **3**.

Sodium salts of the Ln^{III}(**3**) complexes were prepared in H_2O at pH 6.5 (by adding aqueous NaOH) from **3** and the appropriate $Ln^{III}Cl_3$. The excess NaCl was eliminated by electrodialysis.

Ligand **3** has previously been obtained at Dow by a procedure involving the stepwise alkylation of 1,4,7,10-tetraazacyclododecane with α-bromoesters.[13] More recently the same group has reported that the crucial monoalkylation of 1,4,7,10-tetraazacyclododecane can be achieved in very good yield if sufficiently hindered α-bromoesters are used as electrophiles in a 1:1 stoichiometric ratio in $CHCl_3$.[16] In the same paper the crystal structure of a ligand closely related to **2** is also reported.

NMR Characterization. In D_2O, at 25 °C and pD = 7.5, the 400 MHz ^1H NMR spectrum of **3** consists of three well-defined resonances at 8.3 ppm (d, J_{H-H} = 8.6 Hz, 2), 7.8 ppm (d, J_{H-H} = 8.6 Hz, 2), and 5.1 ppm (broadened singlet, 1), corresponding respectively to the meta, ortho, and methylenic protons of the *p*-nitrophenyl acetate group. In addition there are a high number of ill-defined resonances between 4.2 and 2.6 ppm which are attributable to the 22 protons of the 3 acetate and 4 ethylenediamine groups. As the temperature is increased, an overall reduction and sharpening of the resonances in this latter region suggest that a dynamic rearrangement is taking place on the NMR time-scale. Elucidation of this process is better tackled on the basis of the variable temperature (VT) ^{13}C NMR spectra (Figure 1), in particular by looking at the region of the carboxylate absorption. At 275 K (and up to room temperature) four resonances at 178.6, 177.6, 170.9, and 168.7 ppm are detected. The two higher field resonances can easily be assigned to carboxylate groups in which the negative charge is partially removed through the formation of hydrogen bonds with positively charged nitrogen atoms of the macrocyclic ring. In fact, although we have not carried out protonation studies on this ligand, we may reasonably assume that at pH values close to neutrality two of the nitrogen atoms are in the protonated form, as found in other related tetraazamacrocyclic ligands.[17]

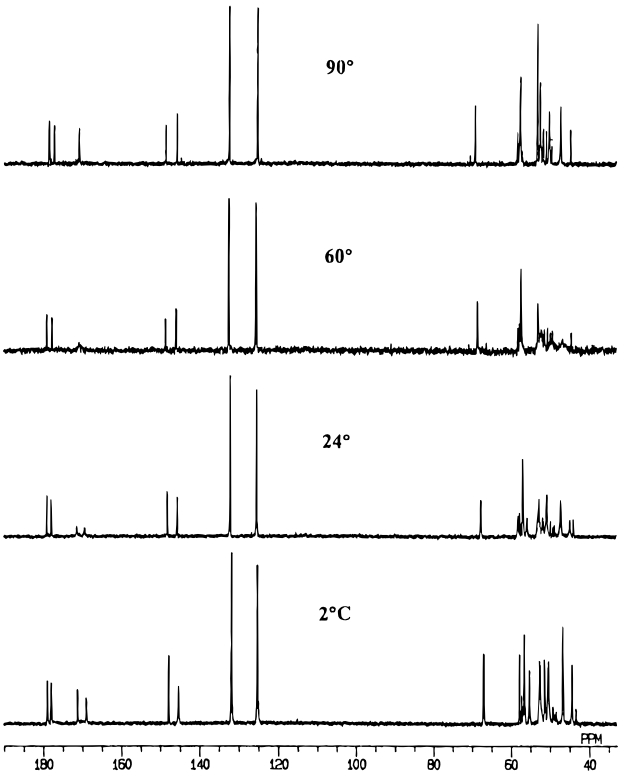

Figure 1. Variable temperature ^{13}C NMR spectra of ligand **3** in D_2O (pD = 7.5).

(16) Kruper, W. J., Jr.; Rudolf, P. R.; Langhoff, C. A. *J. Org. Chem.* **1993**, *58*, 3869.

Thus, the intramolecular interaction of two carboxylate anions with two NH^+ centers results in an overall stereochemical rigidity which in turn leads to a low- symmetry solution structure, as manifested by the inequivalence of both the proton and carbon nuclei in the low-temperature NMR spectra.

As the temperature is increased the two carboxylate resonances at 170.9 and 168.7 ppm broaden, collapse, and then merge into a single resonance at 170.2 ppm. From the chemical shift difference of the two peaks in the low-temperature limiting spectrum and the coalescence temperature we may estimate[18] the free energy of activation for this dynamic process to be $\Delta G^{\ddagger}_{318} = 61.5 \pm 1$ kJ mol^{-1}. Analogous behavior is observed in the methylenic region in which the high-temperature ^{13}C NMR limiting spectrum is consistent with the presence of a mirror plane in the molecule. This may be accounted for in terms of a fast proton exchange over the four nitrogen basic sites of the macrocycle accompanied by a free rotation of the side arms.

Relaxometric Studies of the [Gd(3)]$^-$ Complex. A 1 mM aqueous solution of [Gd(**3**)]$^-$ at 25 °C, pH 7.3, and a proton Larmor frequency of 20 MHz shows a relaxivity of 5.4 mM^{-1} s^{-1}, a value clearly higher than that of the parent compound [Gd(DOTA)]$^-$ (4.7 mM^{-1} s^{-1}). The relaxivity at this frequency, which corresponds to a magnetic field strength within the range of values routinely employed in MRI applications, is normally taken as a direct indication of the ability of a paramagnetic complex to enhance the water proton relaxation rates. Therefore, these data indicate that the chemical modification of one side arm of the DOTA ligand not only does not compromise the relaxation efficiency of the corresponding Gd(III) complex but, on the contrary, it promotes roughly a 15% increase in relaxivity. This result is not surprising if compared with what is known about the magnetic relaxation properties of Gd(III) complexes with both linear and macrocyclic polyamino polycarboxylic ligands.[3] The relaxivity enhancement of the solvent arises from random fluctuations in time of the magnetic dipolar coupling interaction between the unpaired electrons of the Gd(III) ion and the water proton nuclei.[19] This electron−nucleus coupling can be conveniently described as taking place through two distinct mechanisms: (i) *inner sphere*, due to the water molecules present, in number *q*, in the coordination sites of the metal ion, and (ii) *outer sphere*, which involves all the nonbonded water molecules surrounding the complex at a given time (normally, second sphere solvent molecules are not explicitly considered). Modulation of the dipolar interaction, which is responsible for the nuclear spin solvent relaxation, arises from (i) chemical exchange (τ_M is the corresponding correlation time), reorientation of the paramagnetic complex (τ_R), and electron spin relaxation (τ_S) and from (ii) translational diffusion (τ_D) and electron spin relaxation. Moreover, both contributions have a pronounced magnetic field dependence.[3] The data accumulated over the last 10 years allow some general guidelines to be drawn. At the imaging fields normally adopted and at 25 °C the outer sphere water molecules are responsible for a relaxivity contribution of ∼2.0 mM^{-1} s^{-1}, which may account for up to 50% of the total relaxivity for complexes characterized by a *q* value of 1, as is normally the case for compounds such as MRI CAs. The outer sphere component is thus expected to be quite similar for complexes of similar molecular size, as evidenced from its direct dependence from $\tau_D = a^2/D$, where *a* is the minimum distance between the paramagnetic center and the diffusing solvent molecules with values in the range 3.6−5.0 Å[3,4,20] and *D* is the sum of the diffusion constants for the solvent and the metal complex ($D \cong (2.0-3.0) \times 10^{-5}$ cm^2 s^{-2} at 25 °C).[3,4,6,20] Since in the high-field region τ_S plays a negligible role the observed differences in relaxivity can hardly be ascribed to this contribution. The inner sphere component has a value of ∼2.5−3.5 mM^{-1} s^{-1}, for small Gd(III) chelates with $q = 1$ at 20 MHz and 25 °C, depending on the value of the ratio τ_R/r^6, where *r* is the distance between the metal ion and the protons of the coordinated water molecules, within the range 3.0−3.2 Å. In principle, this relaxation mechanism could be influenced by the rate of the chemical exchange of water from the coordination site to the bulk. If the exchange rate is slow with respect to the relaxation rate ($1/T_{1M}$) of the bound water protons, then the relaxation enhancement is partially quenched, as recently observed for a Gd(III) complex with a diamide derivative of DTPA.[6,21] However, this effect is generally not observed at frequencies of 20 MHz or above, near room temperature. Often the condition of fast exchange is rather arbitrarily assumed, even if it could easily be checked by looking at the temperature dependence of the relaxivity. In fact the paramagnetic contribution of the solvent longitudinal relaxation rate is given by the following equation:

$$R_{1p} = \frac{Nq}{55.6} \frac{1}{T_{1M} + \tau_M} \qquad (1)$$

where *N* is the molar concentration of the metal complex. Because of the opposite temperature dependences of T_{1M} and τ_M two limiting cases can be envisaged: (i) *fast exchange* ($T_{1M} \gg \tau_M$); R_{1p} increases by decreasing the temperature and (ii) *slow exchange* ($T_{1M} \ll \tau_M$); R_{1p} decreases by decreasing the temperature. The temperature dependence of the relaxivity of [Gd(**3**)]$^-$ has been investigated between 1 and 70 °C at 20 MHz and pH = 6.8 and clearly shows (Figure 2) a monoexponential decrease of R_{1p} with *T*, as expected for the fast exchange condition. In conclusion, the measured relaxivity value of 5.4 mM^{-1} s^{-1} is likely to be a consequence of a longer τ_R value due to the increased molecular dimension of the complex with consequent decreased tumbling rate, thus implicitly indicating the presence of a single coordinated water molecule. Further

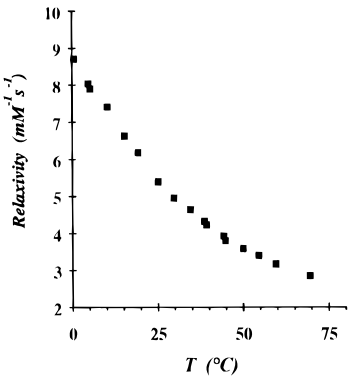

Figure 2. Temperature dependence of the relaxivity for [Gd(**3**)]$^-$ in H_2O at 20 MHz and pH = 7.2.

(17) (a) Desreux, J. F.; Merciny, E.; Loncin, M. F. *Inorg. Chem.* **1981**, *20*, 987. (b) Ascenso, J. R.; Delgado, R.; Fraùsto da Silva, J. J. R. *J. Chem. Soc., Perkin Trans. 2* **1985**, 781.
(18) Friebolin, H. *Basic One- and Two-Dimensional NMR Spectroscopy*, 2nd ed.; VCH: Weinheim, Germany, 1993; pp 293−296.
(19) Banci, L.; Bertini, I.; Luchinat, C. *Nuclear and Electron Relaxation*; VCH: Weinheim, Germany, 1991.
(20) (a) Aime, S.; Batsanov, A. S.; Botta, M.; Howard, J. A. K.; Parker, D.; Senanayake, K.; Williams, G. *Inorg. Chem.* **1994**, *33*, 4696. (b) Hernandez, G.; Brittain, H. G.; Tweedle, M. F.; Bryant, R. G. *Inorg. Chem.* **1990**, *29*, 985.
(21) Gonzàles, G.; Powell, D. H.; Tissières, V.; Merbach, A. E. *J. Phys. Chem.* **1994**, *98*, 53.

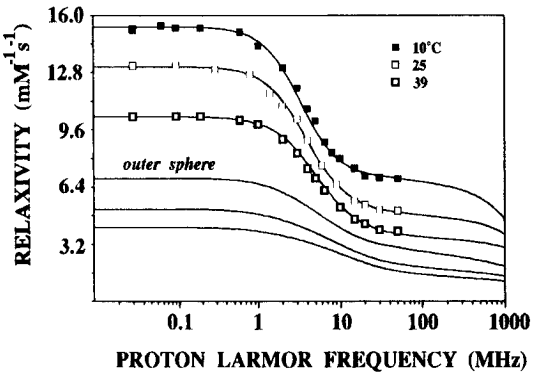

Figure 3. $1/T_1$ NMRD profiles of a 1 mM aqueous solution of [Gd(**3**)]$^-$. The solid curves through the data points were calculated with the parameters of Table 1. The lower curves represent the outer sphere contribution to proton relaxivity.

support to the hypothesis of $q = 1$ comes from the comparison with published data. Tweedle *et al.*[22] have plotted the relaxivity values at 40 °C vs the hydration number q, as determined by luminescence studies, for a series of amino carboxylato Gd(III) complexes of similar size. The plot gave a straight line with an intercept of 2.0 ± 0.3 mM^{-1} s^{-1} (corresponding to the outer sphere component) and a slope of 1.7 ± 0.1 mM^{-1} s^{-1} per coordinated water molecule (corresponding to the inner sphere contribution). We found for [Gd(**3**)]$^-$, at the same temperature, a relaxivity of 4.1 mM^{-1} s^{-1}, a value which clearly indicates the presence of one water molecule in the inner coordination sphere of the complex. Therefore, the introduction of a phenyl group on the methylenic carbon of an acetate arm of the DOTA ligand does not seem to have a negative effect on its potential coordinating ability.

These qualitative observations can be validated by a more thorough analysis of the magnetic field dependence, i.e., by measuring the NMRD (nuclear magnetic relaxation dispersion) profiles.[3,19] This technique allows the full exploitation of the large information content of paramagnetic relaxation. We have measured the NMRD profiles for [Gd(**3**)]$^-$ at 10, 25, and 39 °C (Figure 3) on the field-cycling relaxometer developed by Koenig and Brown, over a wide range of magnetic fields covering the proton Larmor frequencies from 0.01 to 50 MHz. The experimental data can be fitted by the equations describing the inner (Solomon−Bloembergen−Morgan equations[19]) and outer sphere (Freed equation)[23] relaxation mechanisms to give the following set of structural and dynamic relaxation parameters: q, r, a, D, τ_R, τ_M, τ_{S0}, τ_V. The latter two parameters can be entered into the Bloembergen and Morgan equation that describes the field dependence of τ_S and represent its zero field value and the correlation time for the collision of the complex with the solvent molecules, respectively. The number of parameters is too large to give a reliable set of best-fitting values, and thus some of them have to be estimated or derived from other data. According to the discussion above the hydration number q was taken as equal to 1; a and D were given values of 3.6 Å and 2.4×10^{-5} cm^2 s^{-1} (at 25 °C), respectively, which were obtained from the analysis of NMRD profiles for the "outer sphere" complex [Gd(TETA)]$^-$;[24] a value of 80 ± 2 ps for the reorientational correlation time τ_R was calculated at 25 °C by measuring the ^{13}C relaxation rates and NOE factors of some methylenic resonances in the case of the diamagnetic La(III) complex, using a well-established procedure.[25,26] By introducing these values into the paramagnetic equations and by using τ_M, τ_{S0}, τ_V, and r as adjustable parameters, the profiles at 25 °C could be fitted satisfactorily. For the water exchange lifetime τ_M an initial value of 0.2 μs was tentatively assigned, since this was recently calculated by the ^{17}O-NMR technique for DOTA and DTPA complexes.[27] The fitting results have a rather limited depencence from the value of this parameter, despite a better agreement with the experimental data being obtained for a τ_M of 0.1 μs. Finally, when τ_R was also used as a variable parameter the best value obtained was 81 ps. The profiles at 10 and 39 °C were fitted by using the value of 3.02 Å calculated for r at 25 °C and by using τ_R as an adjustable parameter. The best-fitting parameters are reported in Table 1, and the corresponding calculated profiles are shown as continuous lines through the data points in Figure 3. The parameters show the expected temperature dependence: τ_R,τ_M, and τ_V increase with decreasing temperature, while D and τ_{S0} show the opposite behavior. The mean residence lifetime of the coordinated water molecule is much better determined from the data taken at 10 °C since the condition of fast exchange, at least in the low magnetic field region, no longer holds. This results in partial quenching of the relaxivity at low fields, as revealed by a decrease in the ratio of the relaxivities at 0.01 and 20 MHz which passes from 2.4 at 25 °C to 2.1 at 10 °C. In each of the three profiles it is clear that, at any frequency, the inner sphere relaxivity is largely controlled by the reorientational correlation time of the complex whose contribution to τ_C ranges from 71% (0.01 MHz, 10 °C) to 97% (50 MHz, 39 °C). This is well-known for [Gd(DOTA)]$^-$ where it has been attributed to an unusually long electronic relaxation time. However, for [Gd(**3**)]$^-$ it is not obvious since the chemical modification of a carboxylic group into a carboxamide has previously been shown to be accompanied by a drastic reduction of τ_{S0} and therefore of the low-field relaxivity.[5,7] Here the introduction of a phenyl substituent, without changing the type of donor groups of the ligand, has only a limited effect on τ_{S0}, and as a consequence the relaxivity of [Gd(**3**)]$^-$ is higher than the relaxivity of [Gd(DOTA)]$^-$ whatever the magnetic field strength.

As discussed above, one of the main aims in the preparation of [Gd(**3**)]$^-$ was the assessment of the ability of a functionalized paramagnetic carrier to interact with a number of macromolecular substrates, in both covalent and noncovalent modes. A pronounced relaxivity (more exactly the inner sphere component) enhancement is expected as a result of the remarkable lengthening of the reorientational correlation time for the bound form. In this regard, the noncovalent binding is particularly attractive for it ensures both the integrity of the complex and

Table 1. Best Fitting Parameters for the NMRD Profiles of Figure 3[a]

	temperature (°C)		
parameter	10	25	39
τ_{S0} (ps)	271.0(6)	420.0(10)	497.0(12)
τ_V (ps)	15.0(2)	7.4(1)	4.9(1)
τ_R (ps)	113.0(3)	81.0(2)	58.0(2)
τ_M (ns)	282.0(20)	100.0(20)	81.0(30)
D (cm^2 s^{-1}) $\times 10^5$	1.56(0.1)	2.40(0.2)	3.15(0.2)

[a] Numbers in parentheses represent standard deviations in mean parameter estimates on 1000 simulated relaxivity data sets obtained by introducing repeatedly into the experimental data set random errors of 1% and estimating best parameters.

(22) Zhang, X.; Chang, C. A.; Brittain, H. G.; Garrison, J. M.; Telser, J.; Tweedle, M. F. *Inorg. Chem.* **1992**, *31*, 5597.
(23) Freed, J. *J. Chem. Phys.* **1978**, *68*, 4034.
(24) Aime, S.; Botta, M. Unpublished data.
(25) Aime, S.; Botta, M.; Ermondi, G. *J. Magn. Reson.* **1991**, *92*, 572.
(26) Kim, W. D.; Kiefer, G. E.; Maton, F.; McMillan, K.; Muller, R. N.; Sherry, A. D. *Inorg. Chem.* **1995**, *34*, 2233.
(27) Micskei, K.; Helm, L.; Brücher, E.; Merbach, A. E. *Inorg. Chem.* **1993**, *32*, 3844.

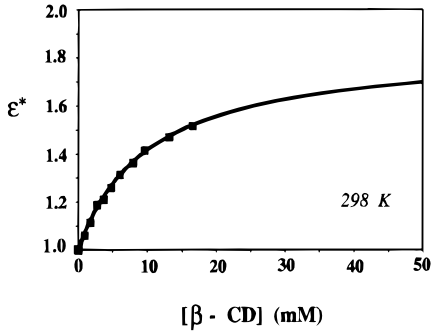

Figure 4. Plot of the proton relaxation enhancement for $[Gd(\mathbf{3})]^-$, at 20 MHz and 25 °C, as a function of β-cyclodextrin concentration. The solid curve was calculated with the binding parameters (K_D and ϵ_b) given in the text.

its stability. We tested the ability of $[Gd(\mathbf{3})]^-$ to interact with the hydrophobic cavity of β-cyclodextrin (β-CD) which was previously found to act as a good model system by forming inclusion complexes of relatively high stability with suitably functionalized Gd(III) complexes.[28] The measurement of water proton relaxation times, at a fixed frequency, provides an easy and accurate tool for determining the strength of the interaction and the extent of the relative relaxation enhancement (ϵ_b) of the inclusion complex. A titration of a 0.5 mM aqueous solution of the $[Gd(\mathbf{3})]^-$ complex with β-CD at pH 7.4 and 25 °C (Figure 4) allowed us to determine a value of 1.7×10^{-2} M for the dissociation constant K_D for the equilibrium

$$\{[Gd(\mathbf{3})]^-/\beta\text{-CD}\} \rightarrow [Gd(\mathbf{3})] + \beta\text{-CD}$$

This K_D value is almost 1 order of magnitude higher than corresponding values obtained for related linear and cyclic polyamino carboxylate Gd(III) complexes containing one or more (benzyloxy)methyl substituents.[28] As expected from the similar size of the two types of inclusion compounds, their relaxivity enhancements are very similar ($\epsilon_b \cong 2$). The larger K_D value of $[Gd(\mathbf{3})]^-$ is presumably a consequence of a poorer fit within the β-CD cavity compared with complexes containing the $CH_2-O-CH_2-C_6H_5$ substituent. In fact, the presence of a nitro group in the para position is expected to strengthen the binding and favor the inclusion complex formation, as found in the case of monosubstituted benzenes.[29] Thus the steric hindrance due to the direct attachment of the aromatic group to the substituted carbon appears to play a major role in controlling the strength of the interaction. Tentatively, we may imagine that the steric crowding does not allow an efficient inclusion of the aromatic ring inside the cyclodextrin cavity and thus the fully exploitation of the hydrophobic interaction.

Solution Structure and Dynamics of $[Ln(3)]^-$ Complexes (Ln = La, Ho, and Yb). A. General Considerations. The basic structural and dynamic features characterizing the aqueous solutions of $[Ln(DOTA)]^-$ complexes are schematically summarized and graphically represented in Figure 5, where A and D represent the square antiprismatic enantiomers and B and C the "inverted" square antiprismatic enantiomeric geometries. The chirality arises from the two opposite elicities in which the achiral ligand can wrap around the metal ion. Interconversion within each enantiomeric pair occurs through inversion of the ethylenic groups and concerted or stepwise rotation of the acetate arms: this process is easily and clearly observed in the VT ^{13}C-NMR spectra since it results in the equilibration at high

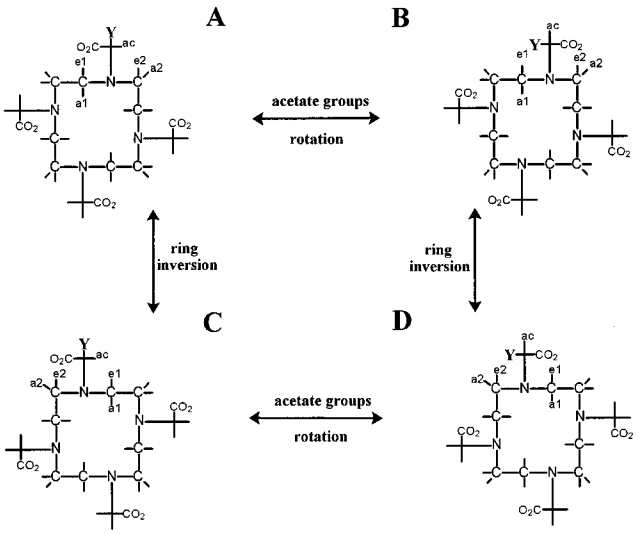

Figure 5. Schematic representation of the two enantiomeric pairs for the $[Ln(DOTA)]^-$ complexes (Y = H) and of the four isomers for the $[Ln(\mathbf{3})]^-$ complexes ($Y = C_6H_5NO_2$) in the case of an *R* configuration of the chiral carbon atom. Labels ac, a, and e identify acetate, axial, and equatorial protons respectively.

temperatures of the two distinct resonances for the ethylenic carbons.[12,30,31] On the other hand, the exchange between the two isomeric forms of the complexes may take place either by rotation of the acetate arms while maintaining the same conformation of the macrocylic ring (A ↔ B; C ↔ D) or by inversion of the ethylenic groups without changing the orientation of the acetate arms (A ↔ C; B ↔ D).[12,31,32]

The substitution of an acetate proton with a group Y (in our case Y = *p*-nitrophenyl) introduces a chiral center in the ligand and a site of asymmetry in the complexes which doubles the number of possible isomeric species in solution. Unlike in the case of $[Ln(DOTA)]^-$ complexes, A and D (and B and C) are no longer enantiomers but diasteromers and are therefore characterized by distinct resonances in their NMR spectra. If the macrocyclic ligand is a racemic mixture, we need to indicate the configuration (*R* or *S*) of the chiral carbon atom of the ligand along with the four arrangements (A−D) of the ligand itself about the metal ion in order to identify completely all the possible stereoisomers. Thus, in the solutions of Ln(III) complexes with monosubstituted derivatives of DOTA we might expect up to eight stereoisomers of the type X_W (X = A−D; W = *R*, *S*). It is worth noting that the mirror image of the isomer A still corresponds to the structural model D, that the enantiomeric form of B corresponds to the structural model C and vice versa, and therefore that the eight stereoisomers constist of four enantiomeric pairs (Figure 6) able to mutually interconvert.

Finally, the lack of axial symmetry removes the signal degeneracy found in the NMR spectra of the $[Ln(DOTA)]^-$ complexes and therefore a large number of resonances are expected for each isomer in the proton (27) and carbon (22) spectra.

$[La(3)]^-$. The ^{139}La NMR spectrum, recorded at 70 °C, shows a single, broad resonance centered at 320 ± 5 ppm. This value is very close to that reported for $[La(DOTA)]^-$ and fully consistent with the empirical rules which ascribe a downfield shift, with respect to the resonance for the aquoion, of 50 and 30 ppm for each coordinated nitrogen and oxygen atom, respectively.[33] This clearly indicates that the substitution does

(28) Aime, S.; Botta, M.; Panero, M.; Grandi, M.; Uggeri, F. *Magn. Reson. Chem.* **1991**, *29*, 923.
(29) Bender, M. L.; Komiyama, M. *Cyclodextrin Chemistry;* Springer-Verlag: Berlin, 1978; Chapter 3.
(30) Desreux, J. F. *Inorg. Chem.* **1980**, *19*, 1319.
(31) Hoeft, S.; Roth, K. *Chem. Ber.* **1993**, *126*, 869.
(32) Vincent, J.; Desreux, J. F. *Inorg. Chem.* **1994**, *33*, 4048.
(33) Geraldes, C. F. G. C.; Sherry, A. D. *J. Magn. Reson.* **1986**, *66*, 274.

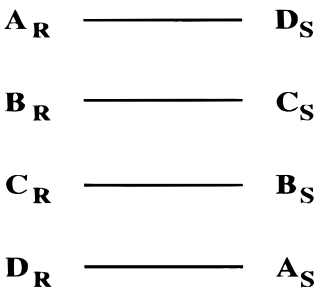

Figure 6. Symbolic representation of the eight possible stereoisomers for [Ln(**3**)]$^-$ complexes. The labels A−D refer to the coordination geometries of Figure 5. Labels *R* and *S* indicate the configuration of the chiral carbon atom of the ligand. The lines connect pairs of enantiomers.

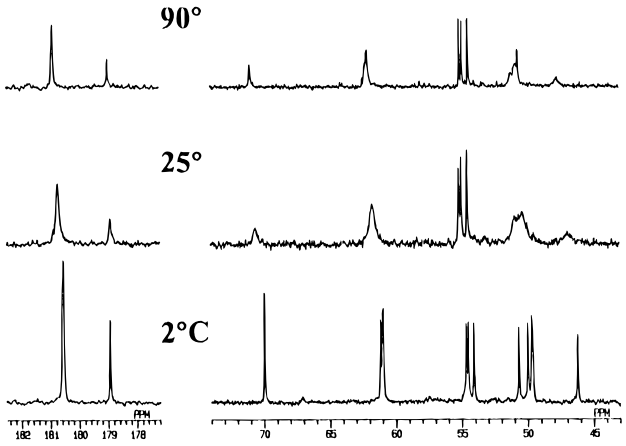

Figure 7. Variable temperature ^{13}C NMR spectra (carbonyl and aliphatic regions only) of [La(**3**)]$^-$ in D_2O (pD = 7.5) at 9.4 T.

not alter the potential octadenticity of the macrocyclic ligand, in full agreement with the relaxometric data. Interestingly, the bandwidth at half-height for [La(**3**)]$^-$ ($\Delta\nu_{1/2}$ = 4950 Hz) is larger than that for [La(DOTA)]$^-$ ($\Delta\nu_{1/2}$ = 3120 Hz),[33] and this directly reflects differences in the transverse relaxation rates which are largely dominated by the quadrupolar mechanism. On this basis such a difference can be easily accounted for by the slightly different values of the corresponding reorientational correlation times and the higher degree of asymmetry for [La(**3**)]$^-$. On the other hand, a broader resonance could also arise from the presence in solution of isomeric species originating NMR signals with small differences in their chemical shift values.

However, the low-temperature limiting ^{13}C NMR spectrum (Figure 7a) shows 12 narrow, distinct peaks in the aliphatic region, corresponding to the 12 different aliphatic carbon atoms of the ligand, thus indicating the presence of just one of the four possible structural isomers. Comparison with the analogous spectrum of the DOTA derivative and a heterocorrelated 2D-COSY experiment allows a rather straightforward assignment of the resonances: carboxylate at 180.7(1), 180.6(2), and 178.9-(1) ppm, aromatic at 148.6(1), 139.7(1), 134.2(2), and 124.3 (2) ppm, acetate at 70.0 (CH), 61.2, 61.0, and 60.9 ppm, and ethylenic at 54.7, 54.5, 54.1, 50.7, 50.0, 49.7, 48.6, and 46.2 ppm. Upon increasing the temperature an overall broadening of all the resonances, particularly marked for those corresponding to the ethylenic ring carbons, is observed over the range 10−40 °C, followed by their sharpening up at higher temperatures (Figure 7). No change in the number of ^{13}C resonances is detected as the process takes place, whereas a differential temperature-dependent behavior is shown by their chemical shift values (relative to the signal of ^{t}BuOH to which a δ = 31.3 ppm was assigned throughout each experiment). For example the chemical shift difference between the high-field carboxylate peaks increases by 0.3 ppm on going from 0 to 90 °C.

The set of ^{1}H NMR spectra essentially reproduce the same basic features and do not add further information. This unusual dynamic behavior can be accounted for by an exchange process involving one major species and one (or more) minor isomer in very low concentration at low temperatures but whose population increases with temperature (endothermic isomerization process). Support for this hypothesis comes from the analysis of the paramagnetic complexes [Ln(DOTA)]$^-$ (Ln = Eu−Yb) that show in their proton NMR spectra two distinct sets of resonances corresponding to two isomeric species. In this case the integration of corresponding pairs of resonances yields a direct estimation of the equilibrium constant for the isomerization process and from its temperature dependence it is evident that the major → minor isomer transformation represents an endothermic process.[34] Finally, it may be noted that the three ethylenic resonances at lower field show a very limited temperature dependence, both in terms of line broadening and chemical shift variation. This can be interpreted as the result of an exchange process between peaks with a small frequency separation and thus characterized by a lower coalescence temperature.

[Ho(3)]$^-$. The remarkable stereochemical rigidity normally encountered with lanthanide(III) complexes of 12-membered tetraazamacrocyclic rings often allows good high-resolution proton NMR spectra to be obtained in the case of highly paramagnetic ions such as Tb, Dy, and Ho. The advantage is that the extremely large chemical shift range (up to 1000 ppm!) characteristic of the spectra of these complexes permits the detection of well-separated peaks for all the nonequivalent protons of the ligand and, in fortunate cases, separate sets of resonances for the different isomeric species present in solution.

The ^{1}H NMR spectrum of [Ho(**3**)]$^-$ in D_2O is shown in Figure 8. The spectrum was recorded for a 0.08 M solution at 25 °C and at 90 MHz since, to minimize severe magnetic field-induced line broadening,[35] it is preferable to operate at low magnetic field strengths. Twenty-two main resonances and a series of other low-intensity peaks cover a range of about 470 ppm. As mentioned above, the lack of a C_4 symmetry axis removes the signal degeneracy found in the spectra of DOTA derivatives and therefore each peak of [Ho(DOTA)]$^-$ is split into a set of four resonances. Thus, in the absence of any fluxional process, we expect to observe 27 distinct signals. On this basis the partial assignment of the spectrum in Figure 8 is possible. Apart from casual overlapping of some resonances (two equatorial protons at −66.0 ppm, one axial and one acetic proton at 62.4 ppm, and two acetic protons at 178.5 ppm), only two peaks for the ortho and meta protons are present at 43.9 and 17.3 ppm, respectively, to indicate the occurrence of a freely rotating aromatic group. We may note, by analogy with DOTA derivatives,[35] that these resonances belong to a species corresponding to a square antiprismatic coordination geometry, i.e., to structural models A or D of Figure 5.

In addition to the main resonances another set of low-intensity signals covering a range of about 300 ppm (from −170 to 125 ppm) is clearly detectable and most likely attributable to the presence of a minor isomeric species. Again, comparison with the spectra of DOTA complexes enables the assignment of some of the resonances to an isomer characterized by an "inverted" square antiprismatic structure of type B or C. Particularly diagnostic in this regard are the four peaks in the −170 to −125

(34) Aime, S.; et al. Manuscript in preparation.
(35) Aime, S.; Barbero, L.; Botta, M.; Ermondi, G. *J. Chem. Soc., Dalton Trans.* **1992**, 225.

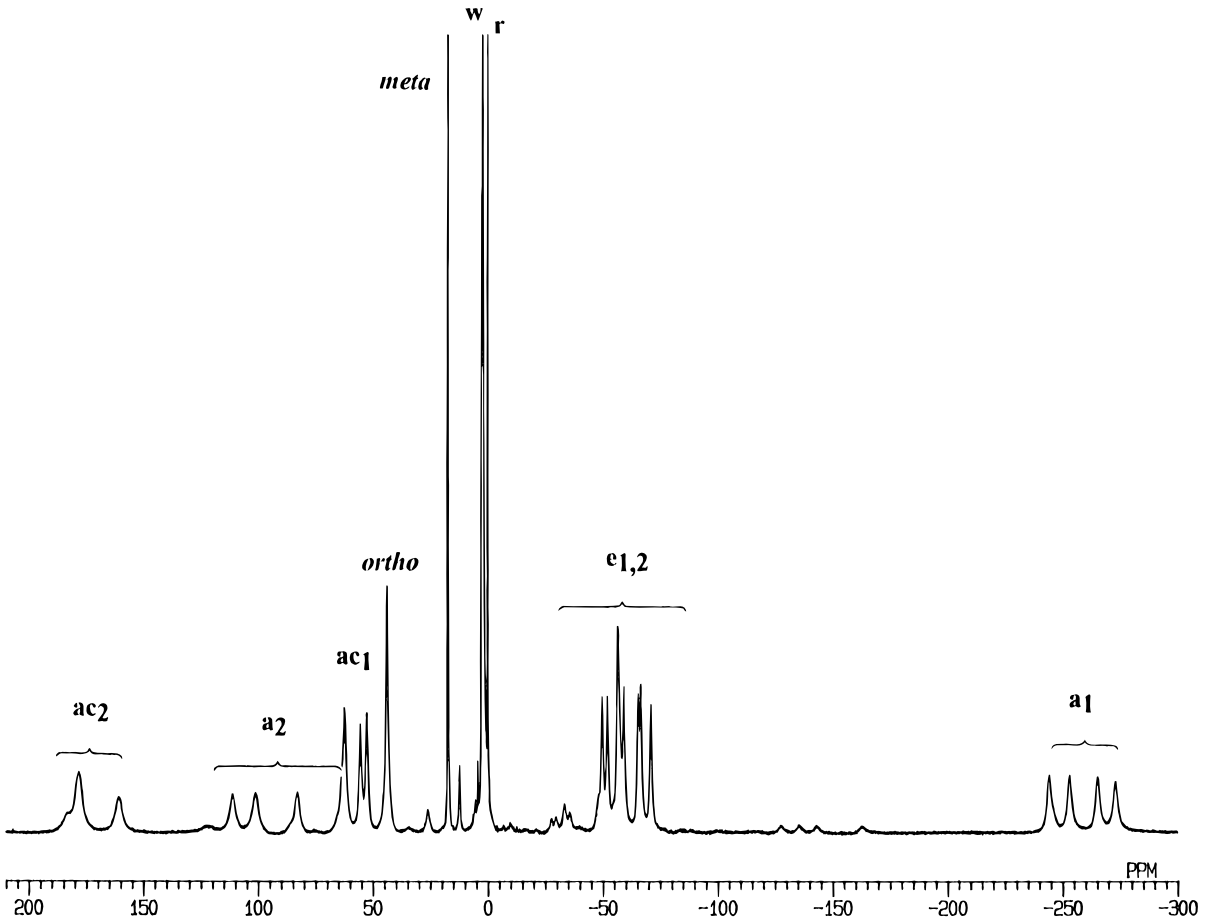

Figure 8. 90 MHz ^{1}H NMR spectrum for a 0.08 M solution of [Ho(**3**)]$^-$ in D_2O at pD = 7.2 and 25 °C. The labels w and r indicate HDO and Bu^{t}OH (internal reference) peaks, respectively. The resonances of the major isomer have been labeled according to the scheme of Figure 5.

ppm range corresponding to four axial protons of the macrocyclic ring. The two isomers have at 25 °C a relative population of 88:12, as determined by integration of corresponding sets of axial peaks at high field, and represent one of the four possible pairs A/B, A/C, D/B and D/C. Further insight into the solution structures of these species can be gained by considering the acetate proton resonances in detail. In [Ln(DOTA)]$^-$ complexes two distinct resonances, ac_1 and ac_2, are detected for the acetate protons for each isomer in the NMR limiting spectrum at low temperature. The two signals differ in their chemical shift values as a consequence of the different location of the protons with respect to the symmetry axis of the complex. They also present rather different bandwidths which reflect differences in the metal−proton distances.[12,35] For the main isomer (enantiomeric pair A/D) of [Ho(DOTA)]$^-$ the "broad" resonance (associated with the proton at a shorter distance) falls at 160.7 ppm and the "narrow" peak of ac_1 at 52.4 ppm. With reference to the schematic models of Figure 5 the "broad" resonance corresponds to the acetate proton close to the macrocyclic ring protons. By increasing the temperature the two signals ac_1 and ac_2 mutually exchange as a result of the enantiomerization processes of the type A ↔ D and B ↔ C. In the monosubstituted derivatives of DOTA the acetate protons give seven distinct resonances in the NMR spectra, divided in two subsets of four and three peaks. The substituent may replace either an ac_1 proton to give enantiomeric pair A_R/D_S (C_R/B_S) or an ac_2 proton to give the other enantiomeric pair D_R/A_S (B_R/C_S). In the first case we would expect to observe a group of four "broad" resonances in the spectrum at low field and a group of three "narrow" resonances at higher field, whereas the opposite situation would occur in the second case. In the spectrum of [Ho(**3**)]$^-$ we clearly observe four "broad" signals in the range 160−185 ppm and three "narrow" peaks in the range 50−65 ppm. This indicates that for this complex the main isomer in aqueous solution corresponds to the enantiomeric pair A_R/D_S. Unfortunately, the acetate signals for the minor isomer are buried under more intense peaks and no inference can be made.

A final comment should be made concerning the close correspondence observed between the proton chemical shift values for the resonances of [Ho(DOTA)]$^-$ and the average values for the related sets of four signals for [Ho(**3**)]$^-$. Since the paramagnetic shift is given by the sum of both contact (through bond) and dipolar (through space) contributions,[36] the close analogy between the ^{1}H NMR spectra of the two complexes means that (i) a very similar unpaired electron delocalization exists in both compounds. This is to be expected because the donor atoms involved in the coordination of the metal ion are the same. (ii) The proton nuclei have quite similar geometrical coordinates. (iii) the principal magnetic susceptibility axis for [Ho(**3**)]$^-$ deviates only slightly from the axis perpendicular to the plane of the four coordinated oxygens. These latter two points can be further confirmed through quantitative analysis of the dipolar shifts which is better accomplished for the Yb derivative for which the contact shift has the smallest theoretical contribution.[36,37]

[Yb(3)]$^-$. The ^{1}H NMR spectrum of this complex (Figure 9) clearly reveals the presence of two isomers in solution at a ratio of 3:1, which roughly corresponds to the isomeric ratio found for [Yb(DOTA)]$^-$[12,31] and confirms the increase of the population of the minor isomer along the lanthanide series. The

(36) Sherry, A. D.; Geraldes, C. F. G. C. In *Lanthanide Probes in Life, Chemical and Earth Sciences: Theory and Practice;* Bünzli, J.-C. G., Choppin, G. R., Eds.; Elsevier: Amsterdam, 1989.
(37) Golding, R. M.; Halton, M. P. *Aust. J. Chem.* **1972**, *25*, 2577.

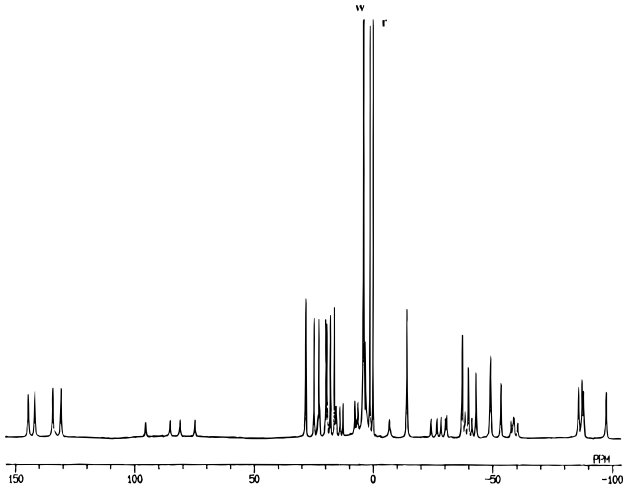

Figure 9. 90 MHz ^{1}H NMR spectrum for a 0.08 M solution of [Yb(**3**)]$^-$ in D_2O at pD = 7.2 and 25 °C. The labels w and r indicate HDO and Bu^{t}OH (internal reference) peaks, respectively. Assignment of the resonances for the major isomer is given in Table 2.

^{1}H resonances of [Yb(**3**)]$^-$ are sharper than those of the corresponding Ho complex, and despite the smaller chemical shift range an even higher number of resonances are observed. The partial assignment of the resonances follows from a comparison with the spectrum of [Yb(DOTA)]$^-$. The spectrum reproduces the same basic features found for the Ho complex: four "broad" acetate peaks at low field and three "narrow" acetate signals at high field. However, in this case a set of four "broad" small intensity resonances is clearly detected for the acetate protons of the minor isomer to indicate for this species a solution structure of the type C_R/B_S. To confirm these qualitative hypotheses on the solution structures of Ho and Yb complexes with ligand **3** the ^{1}H NMR spectrum was quantitatively and carefully analyzed as previously reported for [Yb(DOTA)]$^-$.[12] The analysis was restricted to the resonances of the principal isomer since only in this case was it possible to clearly distinguish each of the 25 different peaks. Unlike the axially symmetric DOTA complex, the analysis of the dipolar-induced shift on the proton resonances by the paramagnetic metal ion in [Yb(**3**)]$^-$ has to be based on the use of the complete form of the dipolar equation:[36]

$$\delta\nu_i = D_1\frac{3\cos^2\theta - 1}{r^3} + D_2\frac{\sin^2\theta\cos 2\phi}{r^3} \qquad (2)$$

where D_1 and D_2 represent the magnetic susceptibility factors and r, θ, and ϕ are the polar coordinates of the ligand nucleus i with respect to the magnetic susceptibility axes of the complex.

The r distances between the paramagnetic center and a given proton atom were independently evaluated by exploiting the Curie contribution to the relaxation rates of the proton resonances for the related [Ho(**3**)]$^-$ complex, according to a well-established procedure.[35] In this case we measured the longitudinal relaxation rate $1/T_1$ at three magnetic field strengths (2.1, 6.3, and 9.0 T) at 25 °C. If the value of the molecular reorientational correlation time τ_R is known, then, from the field dependence of the relaxation rate, the distances r can be evaluated according to the equation

$$\frac{1}{T_1} = \frac{4\gamma^2\mu_{\text{eff}}{}^2}{3r^6}\tau_S + \frac{\gamma^2\mu_{\text{eff}}{}^4H_0{}^2}{5(3kT)^2r^6}\left[\frac{6\tau_R}{1+\omega_H{}^2\tau_R{}^2}\right] \qquad (3)$$

The τ_R value of 81 ps derived from the analysis of the NMRD profile for the Gd complex was used. The data were taken for the Ho complex since its higher value of the effective magnetic moment results in a larger Curie spin contribution to the relaxation rate and therefore in more accurate results. Once the distances for the different protons have been calculated, from the dipolar contribution to the relaxation rate (first term of eq 3), the value of the electronic relaxation time τ_S can be obtained.[35] The very similar τ_S value, 0.12 ± 0.2 ps, calculated from the data for the different peaks provides an internal check to validate the accuracy of the procedure. This value is also rather similar to those calculated for [Ho(DOTA)]$^-$ (0.15 ps)[35] and [Ho(H$_2$O)$_9$]$^{3+}$ (0.27 ps)[38] to confirm that this parameter is rather insensitive to the chemical environment of the metal ion. The calculated distance values were used as input adjustable parameters in the best-fitting procedure.

Table 2. Calculated and Experimental Proton[a] NMR Shifts for the A_R/D_S Enantiomeric Pair of [Yb(**3**)]$^-$ at 5 °C and Best Fitting Parameters

proton	$\delta\nu_{calc}$	$\delta\nu_{sper}$	proton	$\delta\nu_{calc}$	$\delta\nu_{sper}$
H_1	160.5	157.3	H_{13}	−43.0	−48.1
H_2	155.2	154.3	H_{14}	−45.0	−44.9
H_3	151.0	157.3	H_{15}	−45.5	−45.2
H_4	146.4	142.2	H_{16}	−46.0	−50.5
H_5	30.5	29.4	H_{17}	−52.5	−58.1
H_6	29.7	29.0	H_{18}	−54.8	−58.1
H_7	30.1	25.3	H_{19}	−62.5	−62.6
H_8	25.1	23.0	H_{20}	−94.6	−98.9
H_9	24.4	19.7	H_{21}	−95.5	−100.2
H_{10}	22.0	19.4	H_{22}	−101.0	−101.2
H_{11}	19.1	17.8	H_{23}	−104.0	−111.9
H_{12}	18.1	15.7			
D_1	5254	D_2	-250	R	0.045

[a] Labeled according to Figure 10.

On the basis of the close similarity between the chemical shifts of [Yb(**3**)]$^-$ (when for each type of proton the average of the four resonances is considered) and those of [Yb(DOTA)]$^-$ which is indicative of a close similarity of the corresponding structures and which further reinforces the considerations made before for the Ho derivative, our analysis of the dipolar shift was restricted to the two square antiprismatic structures, A_R and D_R, as starting models. As the method is based on comparing experimental shifts with those calculated through eq 2, by using geometrical factors extracted from the model structures, we used a procedure that is able to modify systematically the internal coordinates of the model to get the best agreement between calculated and experimental shifts. Different constraints were used (suitable range of variability for distances, dihedral, and bond angles) with the aim of maintaining a real physical meaning for the model. As suggested previously, to test the quality of the obtained model for any orientation of the magnetic axes we used an agreement factor R, defined as

$$R = \frac{\sum_i(\delta\nu_i^{\text{calc}} - \delta\nu_i^{\text{exp}})^2}{\sum_i(\delta\nu_i^{\text{exp}})^2} \qquad (4)$$

where δ^{calc} is the chemical shift value calculated with eq 2 for a given proton for each isomeric structural model for a given orientation of the magnetic axes.

As expected, a very good agreement factor, $R = 0.045$, was obtained upon fitting the more intense set of resonances to the structural model A_R of Figure 5. The data analysis was performed on the spectrum recorded at 5 °C to ensure, as much as possible, the occurrence of static structures. The comparison

(38) Bertini, I.; Capozzi, F.; Luchinat, C.; Nicastro, G.; Xia, Z. *J. Phys. Chem.* **1993**, *97*, 6351.

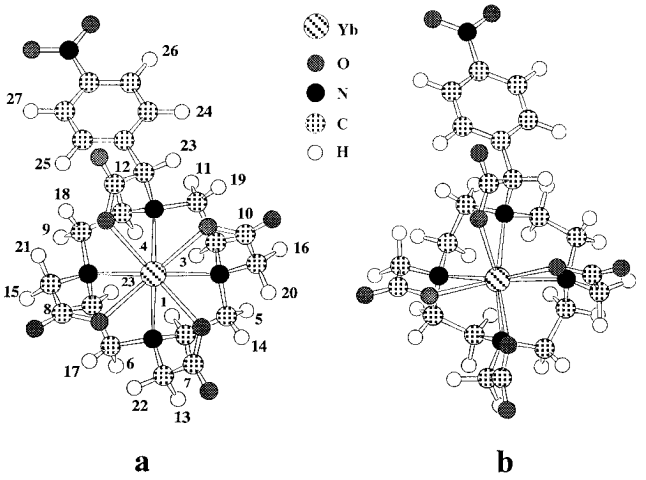

Figure 10. Structures of the two isomers present in the aqueous solutions of $[Yb(\mathbf{3})]^-$: (a) major isomer (enantiomer A_R, calculated by analysis of the dipolar shifts) with proton labeling scheme and (b) minor isomer (enantiomer C_R).

Scheme 2

A↔B	A↔C
a1↔a1	a1↔e2
e1↔e1	e1↔a2
e2↔e2	e2↔a1
a2↔a2	a2↔e1

between observed and calculated shifts is reported in Table 2 and the structure (for the enantiomer A_R) derived from the best-fitting procedure is shown in Figure 10a. An analogous procedure for the minor isomer does not result in a good fit because of the incomplete spectral assignment arising from the fact that several peaks are masked by the more intense resonances of the principal isomer. However, further insights into the structure of this species are provided by a simple 2D-EXSY experiment which clarifies the details of the exchange pathway between the two isomers. According to the scheme of Figure 5 the enantiomer A_R can interconvert either to B_R through the motion of the acetate arms or to C_R through the inversion of the conformation of the ethylenediamine groups. If we focus our attention on the macrocyclic ring protons we see that the two exchange pathways interconvert different proton pairs according to Scheme 2.

The ^{1}H 2D-EXSY spectrum of $[Yb(\mathbf{3})]^-$ reported in Figure 11 clearly shows all the proton connectivities which correspond nicely to case A ↔ C of Scheme 2.

In conclusion the two isomers found in the aqueous solution of the La, Ho, and Yb complexes of ligand **3** correspond to structural models A and C (Figure 10). In both structures the substituent has replaced the same type of acetate proton, the one located at a longer distance from the metal ion and pointing outward from the coordination cage. This minimizes the steric interaction of the bulky *p*-nitrophenyl group with the macrocyclic ring protons and in this regard free rotation of the aromatic substituent in these species has been observed. Besides structural selectivity the steric factors also play a major role in controlling the dynamics of the complexes. Unlike the DOTA case the interconversion process between the two isomers involves only a rearrangement of the macrocycle: the steric encumbrance of the substituent does not allow the acetate arm to slide over the surface of the coordination cage.

Conclusions

The relaxometric, structural, and dynamic properties of aqueous solutions of lanthanide(III) complexes of the *p*-

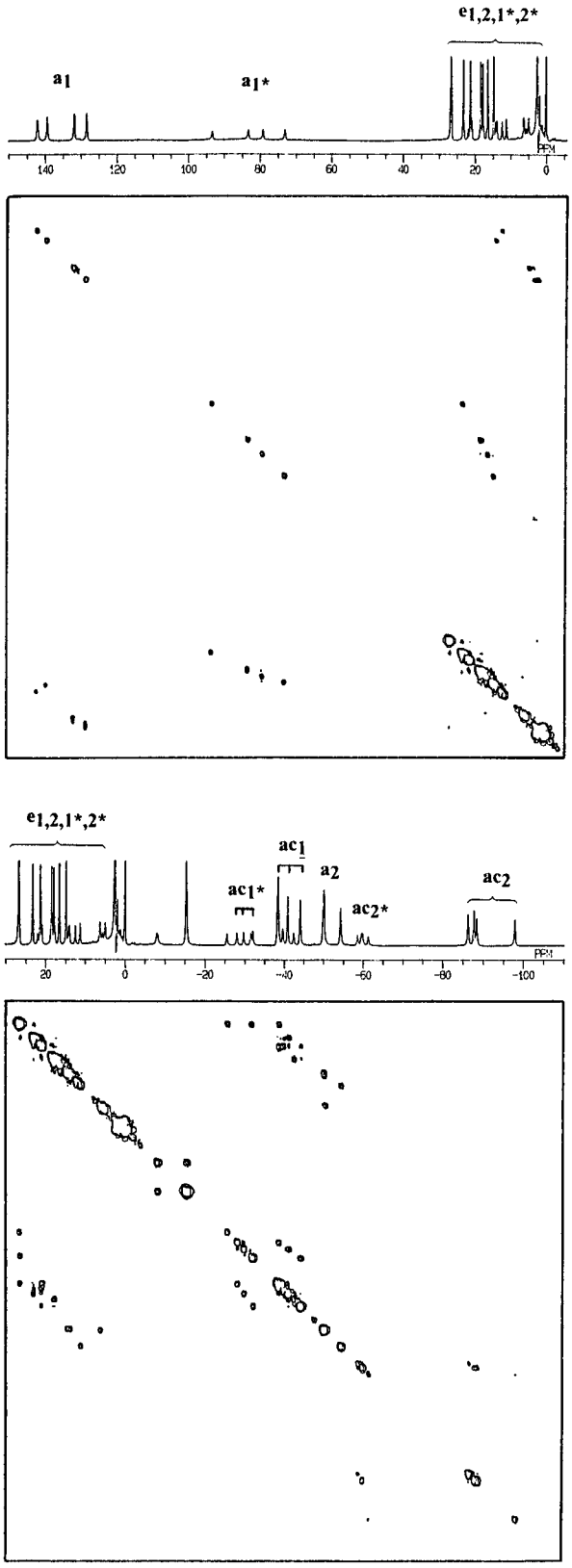

Figure 11. Expanded regions (top, low field; bottom, high field) of the 400 MHz 2D-EXSY spectrum for a 0.08 M solution of $[Yb(\mathbf{3})]^-$ in D_2O at pD = 7.2 and 25 °C with a mixing time t_m = 5 ms and presaturation of the HDO peak. Data were collected with 1024 points in F_2 (128 scans; 112 000 Hz) and 512 points in F_1, using a delay between pulses of 0.5 s. Data were processed using a sine square-bell function in F_1 and F_2. The asterisks indicate the resonances of the minor isomer. For clarity reasons the four axial peaks of the minor isomer in the range −25 to −43 ppm have not been labeled.

nitrophenyl derivative of DOTA have been investigated by low- and high-resolution NMR techniques. The relaxivity of the Gd complex is higher than that of $[Gd(DOTA)]^-$ over a wide range of magnetic field strengths as a result of a slight increase of the molecular dimension and a negligible decrease of the electronic relaxation time of the metal ion. The relaxivity is enhanced slightly after formation of an inclusion compound with β-cyclodextrin, although steric crowding at the substituent site has a negative influence on the strength of the interaction as indicated by the high value of the calculated dissociation constant.

Interesting effects due to chemical modification of the parent DOTA ligand have been observed on the solution structures and dynamics of the complexes. While four enantiomeric pairs are expected in the solution of monosubstituted DOTA derivatives, only two are actually observed. These differ in the relative orientation of the two square planes formed by the donor atoms, and their structures can be described as square antiprismatic and "inverted" square antiprismatic, respectively. On the other hand, in both isomers the substituent is located in a strictly analogous position, pointing outward from the coordination cage, a position that reduces steric repulsion with the protons of the macrocyclic ring. Accordingly, the two isomers mutually interconvert through a concerted rotation of the four ethylenediamine rings, as evidenced by a 2D-EXSY experiment for the Yb(III) complex. The acetate groups are not involved in this dynamic process. Such steric control of the structural and dynamic features of the $[Ln(\mathbf{3})]^-$ complexes could likely be removed by introducing a spacing aliphatic chain between the bulky aromatic group and the substituted acetate group. In this case we should be able to observe all four isomeric species and, more importantly, the increased motional freedom and reduced steric constraint of the pendant substituent should favor the creation of noncovalent interactions with suitable substrates and thus the optimization of the relaxivity of the Gd(III)-chelate for different biomedical applications.

IC950981U